SYNTHETIC NI GOETHITE AND HEMATITE: REPRODUCING HOSTS FOR NICKEL MINERALIZATION IN NI-LATERITES

M. A. WELLS[#] AND R. J. GILKES[*]

[#]*CRC LEME, CSIRO Exploration and Mining, c/- University of Canberra, Belconnen ACT, 2616*
[*] *Department of Soil Science and Plant Nutrition, University of Western Australia, Nedlands, 6907.*

ABSTRACT

Incorporation of Ni within synthetic goethite and hematite was investigated by x-ray diffraction (XRD) and acid dissolution analysis. Goethites synthesized by the oxidation of mixed Fe^{2+}-Ni^{2+}-chloride solutions at room temperature and pH 6-7 uniformly incorporated up to 10mole% Ni. Goethites prepared at ambient temperature and pH >12 incorporated 5-6 mole% Ni at the surface of crystals. Differences in the extent and homogeneity of Ni incorporation appear related to the different synthesis conditions and kinetics of goethite crystallization. Incorporation of the larger Ni^{2+} ion resulted in anisotropic distortion of the goethite unit-cell. The unit-cell b-dimension increased linearly as Ni substitution increased whereas the a- and c-dimensions remained unchanged.

Hematite prepared from coprecipitated Ni-ferrihydrite gels at pH 7-8 and 90°C, uniformly incorporated up to 6 mole% Ni. Unit-cell parameters increased linearly with increasing Ni substitution indicating the replacement of Fe by Ni within the hematite structure.

Key words: Nickel laterites, Goethite, Hematite, Ni-substitution

INTRODUCTION

Lateritic nickel deposits form by the chemical weathering of ultramafic Ni-host rocks. Most Ni-laterites of commercial significance appear to have formed from serpentinized peridotite containing forsteritic olivine as the primary Ni source (Burger, 1996).

Nickel laterite profiles are zoned and consist of a general sequence from the bedrock to surface of: unweathered ultramafic; saprolite zone; clay zone; ferruginous zone and thin soil cover (Burger, 1996). Lateritic Ni-deposits can be classified into three sub-types depending on the mineralogy of the main Ni-bearing phases:

Type-A deposits: These are dominated by 'garnierite-like' phases, which are essentially hydrated Mg-Ni-silicates (as characterized by some of the New Caledonian deposits).

Type-B deposits: These consist mainly of smectite (montmorillonite, nontronite) and chlorite as the main Ni-hosts typical of the Bulong and Murrin Murrin Ni deposits, Western Australia.

Type-C deposits: The main Ni-hosts are Fe-oxide/oxyhydroxide minerals, usually goethite and hematite, characteristic of the Cawse Ni-laterite deposit, Western Australia.

In the Yilgarn of W. A. only Type-B and Type-C deposits have been described. Within the ferruginous zones of Type-B, and in particular Type-C deposits where goethite is the dominant Fe-phase, Ni contents generally range from 0.5 to 1.5 % (Golightly, 1979; Schellmann, 1983). However, Nahon et al. (1982) report NiO contents of 1.5-2.5 % (1.2-2.0 % Ni) in ferruginous layers of Ivory Coast Ni-laterites and compared these data to Ni contents for oxidized zones of other Ni-laterites (mainly mixtures of Type-B and Type-C) with Ni contents as high as 3.5% (2.8 % Ni).

The nature of the Ni-goethite association is not well understood, although it is generally thought that Ni is incorporated within the structure of goethite and occupies Fe^{3+} sites in octahedral coordination (Golightly, 1979, 1981; Nahon *et al.*, 1982; Schellmann, 1983, Burger, 1996). These studies, however, have not provided direct evidence for the isomorphous substitution of Fe by Ni and a degree of confusion exists about a possible mechanism as evidenced by the work of Burger (1996) who considered that Ni^{2+} replaced Fe^{2++} within goethite.

The scavenging abilities of hematite, and in particular goethite for foreign cations are well known in the soil science literature. Associations of a range of elements including Al, Ti, Cr, Mn, Co, Cu, Zn, Pb, Ge, Ga, Mo and Cd have been reported for both natural and synthetic goethite and hematite (Norrish, 1975; Fitzpatrick *et al.*, 1978; Bernstein and Waychunas, 1987; Kuhnel, 1987. Elements such as Al and Cr have also been reported to be present in goethite in the oxidized zones of Ni-laterite deposits (Elias et al., 1981; Golightly, 1981; Nahon et al., 1982). Later work has since confirmed the replacement of Fe^{3+} by several metals within goethite, including: Mn - Stiers and Schwertmann (1985), Cr - Schwertmann *et al.* (1989), V - Schwertmann and Pfab (1994), and Co - Gasser et al. (1996).

The acid dissolution of limonitic Ni-ores (Schellmann, 1983) and synthetic Ni-goethites (Lim-Nunez and Gilkes, 1987) has provided indirect evidence for Ni replacing Fe within goethite. Gerth (1990) confirmed the replacement of Ni for Fe by x-ray diffraction (XRD). Changes in the unit-cell dimensions of synthetic goethites were linearly and positively related to the level of Ni substitution to a maximum of 6 mole%. Lim-Nunez and Gilkes (1987) also provided indirect evidence for the replacement of Fe by Ni in hematite. Direct evidence for the isomorphous substitution of Fe within hematite has not been demonstrated.

The present study was, therefore, undertaken to provide evidence for the incorporation of Ni within hematite and a maximum limit of substitution. Previous investigations of synthetic Ni-substituted goethite have been limited in only examining goethite produced at very high pH (i.e. >10-12) and/or at elevated temperatures, usually in the range 50-70°C (Lim-Nunez and Gilkes, 1987; Gerth 1990). These conditions are unlikely to occur in soils or weathering profiles. The present study was also, therefore, undertaken to synthesize Ni-substituted goethites under conditions more likely to occur in nature (i.e. neutral pH and ambient temperature), and to establish a maximum limit of Ni-substitution.

METHODS

Synthesis of goethite and hematite

Synthetic goethites were prepared using two common methods:

S1-series: Fe^{2+}- and Ni^{2+}-chloride solutions were mixed, to give a total cation concentration of 0.1M, with a $NaHCO_3$ buffer solution to provide a 5 mmole/L excess of that needed for complete hydrolysis of Fe^{2+} and Ni^{2+}. The solutions were oxidized with compressed air at approximately 35-40 ml/min. As oxidation proceeded pH remained buffered at 6.5-6.8 rising to pH 8.2 at the completion of oxidation; generally taking 1-2 days.

S2-series: 600ml of 5M KOH was added to 1.0L solutions of Fe^{3+}- and Ni^{2+}-nitrate of total cation concentration of 1.0M. Deionized water was added to increase solution volume to 4.0L. The precipitate was then aged at 25°C for 16 days. During ageing the precipitate was mixed by end-over-end shaking in plastic containers to avoid contamination by Si and solution pH maintained at >12.

The products of both goethite series were centrifuged/washed with three, 100 ml lots of deionized water (DI) before drying at 40°C from a final wash with acetone prior to further analysis.

Hematite was prepared from ferrihydrites coprecipitated from mixed Fe^{3+}-Ni^{2+}-nitrate solutions via the addition of 4M NH_4OH until in about 30% excess of the stoichiometric quantity required to precipitate the Ni-ferrihydrites. Ferrihydrite gels were collected by centrifugation, washed with three lots of 200ml deionized (DI) water, transferred to 1.0L stoppered, glass reagent bottles and resuspended with 900 ml DI water to pH 7.5-8.0. The suspensions were aged at 90°C for 14 days. After ageing the solid material was washed with DI water and dried from acetone at 40°C.

Goethites and hematites were prepared with initial, Ni/Ni + Fe, molar ratios of 0, 0.03, 0.05, 0.07 and 0.15.

S1- and S2-series goethites consisted mainly of monomineralic goethite. Reevesite, $Ni_6Fe_2(CO_3)(OH)_{16}$, was present for S1-goethite prepared with a nominal Ni/Ni + Fe ratio of 0.15. Trace amounts of goethite were detected for hematite prepared with a molar ratio of 0.03 Ni. Reevesite and the goethite contaminants were completely removed by treatment with ammonium oxalate (i.e. were not detected by XRD), so that all the products investigated in this research consisted only of goethite or hematite.

CHEMICAL ANALYSIS

Residual ferrihydrite and any unincorporated Ni adsorbed on the surface of goethite and hematite was removed by treatment with two, 60 minute acid (pH 3 0) ammonium oxalate extractions in the dark (Schwertmann, 1964; McKeague and Day, 1966) using a sample to solution ratio of 1:200 (Parfitt, 1989) Samples were washed with DI water to remove any salts and again dried from acetone before analysis.

Chemical compositions of goethite and hematite were determined for ammonium oxalate-treated samples, following complete dissolution of 50 mg samples in 30 ml of 32% HCl Fe and Ni contents of the solutions were determined by atomic absorption spectrometry (AAS).

X-RAY DIFFRACTION (XRD)

XRD analysis was conducted using a Philips PW 1050 vertical goniometer with 1° receiving and divergence slits, and graphite monochromator with Cu Kα radiation XRD patterns were obtained by step scanning back-filled powder mounts, with 10 % NaCl added as an internal standard, at 0 3° 2θ/min in 0 01° 2θ steps for the accurate measurement of spacings and line broadening determinations

Goethite and hematite reflections were also corrected for shifts in line position due to small particle size where the width at half height (WHH), corrected relative to the NaCl standard, was >0 6°2θ (Schulze, 1984) The calibration curves of Schulze (1982) and Helge Stanjek (pers. comm) were used for goethite and hematite, respectively

Unit-cell edge dimensions for goethite and hematite were calculated using a crystallographic least squares template program (Novak and Colville, 1989) Unit-cell edge lengths for hematite was calculated from corrected positions of the 012, 104, 110, 113, 116, 018, 214 and 300 lines Unit-cell edge lengths for goethite were determined from the corrected positions of two sets of reflections. For S2-goethites unit-cell edge lengths were derived from the:

1. 110, 130, 111 and 140 reflections
2. 020, 110, 120, 130, 021, 111, 121, 140, 160 and 250 reflections

For S1-goethites only the positions of the 110, 130, 111 and 140 reflections could be precisely determined due to line broadening of the other reflections

ELECTRON MICROSCOPY

Transmission electron microscopy (TEM) was performed using a Philips 430 analytical transmission electron microscope (ATEM) operating at 300kV Samples were prepared for TEM examination by air drying suspensions of oxalate-treated goethite and hematite onto carbon-coated copper grids.

Selected area diffraction (SAD) patterns of single crystals together with the typical composite lath morphology of goethites confirmed the orientation of the a-axis parallel to the electron beam (Cornell *et al*, 1983). As a consequence of this morphology, TEM examination only allowed changes in crystal size along the b-and c-directions (i e crystal width and length, respectively) to be observed. The typical plate-like morphology of hematite results in the c-axis (i e crystal thickness) being oriented parallel to the electron beam TEM therefore, only permits changes in crystal growth along the a-direction (i e width) to be examined.

ACID DISSOLUTION

The uniformity of Ni incorporation within goethite and hematite was investigated by acid dissolution in HCl 10mg samples of oxalate-treated goethite and hematite per 22 ml of AR grade 1M HCl were placed in 25 ml polythene vials Sample vials were shaken in a controlled environment incubator shaker at 400 cycles per minute (cpm) at 60°C A one-half to 1 0 ml aliquot was withdrawn from the suspensions at selected times using a 3 ml plastic syringe and filtered using 'Millipore' 0 22 µm cellulose nitrate membranes Iron and nickel concentrations were determined by atomic absorption spectrometry (AAS).

The sample:solution ratio and shaking speeds were selected to ensure that dissolution was not diffusion controlled and independent of the sample mass to acid volume ratio (Cornell *et al*, 1974)

RESULTS AND DISCUSSION

CHEMICAL ANALYSIS

The Ni contents of oxalate-treated S1- and S2-series goethites and hematites, plotted against their nominal Ni contents are shown in Figure 1. For S1 and S2 goethites chemically determined Ni contents were less than nominal Ni concentrations. The proportion of Ni incorporated within goethite decreased in a curvilinear fashion with S1 goethites incorporating more Ni than S2 goethites (Figure 1). The maximum level of Ni-substitution for S2-goethite of about 6 mole% is similar to the maximum amount of 5-6 mole% incorporated in goethite produced under similar conditions of high pH by Gerth (1990). This amount is approximately half the maximum level of 10 mole% Ni incorporated into S1 goethites in the present study. This result may be related to differences in the mechanisms of goethite formation for the two different methods of synthesis used in the present study.

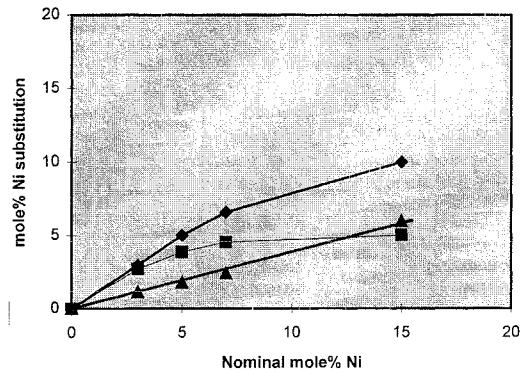

Figure 1. *Mole% Ni-substitution in oxalate-treated (◆ S1- and (■ S2-goethites, and (▲ hematites. Regression analysis for Ni-hematites y = -0.16 + 0.40% Ni (r^2 = 0.995***)*

MECHANISMS OF NI-GOETHITE FORMATION

Goethite synthesis under alkaline conditions (i.e. pH>12) involves dissolution of the amorphous ferrihydrite gel and precipitation of goethite (Schwertmann and Fischer, 1966; Fischer and Schwertmann, 1975). Goethite precipitation occurs via formation of crystal nuclei fed by $Fe(OH)_4^-$, the predominant Fe-species at high pH (Baes and Mesmer, 1976), to the ends of $Fe(O,OH)_6$ octahedral chains along the goethite c-direction (Cornell et al., 1983). The degree of congruency of ferrihydrite dissolution may influence the extent of metal substitution in goethite (Giovanoli and Cornell, 1992). Ions released into solution can then be incorporated within the growing goethite as crystals form. However, the metal ion species presented to growing goethite crystals would be modified by the aqueous chemical conditions e.g. pH and anion system.

Under alkaline conditions (pH>12) Ni occurs as the $Ni_4(OH)_4^{4+}$ ion, which is thought to have a cubic structure with interpenetrating Ni_4 and $(OH)_4$ tetrahedra (Baes and Mesmer, 1976). Although electrostatic considerations favour absorption of $Ni_4(OH)_4^{4+}$ onto crystallizing goethite nuclei, the complex nature (and size?) of the tetramer may inhibit extensive incorporation. This is despite the strong preference of Ni for octahedral sites in both high and low spin state electron configurations (Cotton and Wilkinson, 1980).

Goethite synthesis via the oxidative hydrolysis of Fe^{2+}-Ni^{2+}-chloride solutions buffered at pH 6-7 (i.e. S1 goethites) involves formation of intermediate 'green-rust' complexes (Bernal *et al.* 1959). Weakly hydrolyzed metal ions modify the oxidation of these green-rusts by forming blue-green, pyroaurite compounds which consist of brucite-like $Mg(OH)_2$ layers containing both M^{2+} and M^{3+} cation sites interlayered with anions and H_2O molecules (Taylor and McKenzie, 1980). The M^{2+} sites can be occupied by ions such as Mn^{2+}, Fe^{2+}, Ni^{2+}, Co^{2+}, Mg^{2+} and Zn^{2+}, whilst the M^{3+} sites may be filled by Al^{3+}, Fe^{3+}, Mn^{3+} or Co^{3+} (Taylor and McKenzie, 1980).

At neutral pH, $Ni^{2+}(aq)$ occurs in equilibrium with $Ni(OH)_2$ (Baes and Mesmer, 1976). Compared to S2-goethites prepared at high pH, weakly hydrolyzed Ni^{2+} ions may be more easily accommodated within the intermediate green-rust phase, resulting in a higher level of Ni substitution (10 mole%) for goethites prepared at near neutral pH.

The conditions of synthesis of S1-goethites, involving oxidation of mixed Fe^{2+}-Ni^{2+}-intermediate complexes at neutral to slightly alkaline pH, more closely resemble the conditions under which Ni-laterites form in nature (Schellmann, 1983) than the very high pH conditions for the synthesis of S2-goethites.

The level of Ni incorporated into hematite increased uniformly as the nominal Ni concentration increased to a level of about 6 mole% Ni (Figure 1) but substitution was about one-third of the nominal amount for each value. A maximum limit of Ni substitution was not shown for hematites prepared in the present study. Further study is required to determine the maximum extent of Ni-substitution in hematite.

UNIT-CELL DIMENSIONS OF GOETHITE AND HEMATITE

Unit-cell a- and c-dimensions of S2-goethites calculated using the second set of diffraction lines show a much smaller range of 4 619 - 4 630 Å for *a* and 3 021 - 3 024 Å for c as compared to the range of 4 623 - 4 643 Å for a and 3 016 - 3 025 Å for c derived from positions of the 110, 130, 111 and 140 lines (Table 1) This is because of the increase in precision from the use of many more diffraction lines to calculate goethite unit-cell edge lengths The magnitude of *a* and c values for S2-goethites calculated using the second set of diffraction lines are similar to published values of *a* and c for Ni-goethites produced at high pH (Gerth, 1990)

Unit-cell a- and c-dimensions for S1- and S2-goethites, therefore, remained essentially unchanged as Ni substitution increased (Table 1) Lim-Nunez (1985) and Gerth (1990) also observed that the a- and c-dimensions of goethites produced under alkaline conditions and incorporating up to 5mole % Ni, were not affected by Ni substituting for Fe The spacing of the 110 reflection of goethites from limonitic Ni-ores was also unrelated to Ni contents up to 1 5% NiO (Schellmann, 1983)
However, in this study the b-dimension of S1- and S2-goethites was positively related (r^2 of 0 87 and 0 83, respectively) to increasing amounts of Ni (Figure 2) indicating the isomorphous replacement of Fe by Ni within goethite The unit-cell b-dimension of S2-goethites calculated from corrected positions of the 020, 110, 120, 130, 021, 111, 121, 140, 160 and 250 lines was also linearly and positively related to increasing amounts of Ni; b = 0 0047 %Ni + 9 962 (r^2 = 0 881**)

Values of the slope (i e Å/mole% Ni) for plots of b, calculated from the 110, 130, 111 and 140 lines, versus mole% Ni of 0 0049 and 0 0057 for S1- and S2-goethites, respectively, are similar to the published value of 0 00338 for Ni-goethites produced under high pH (Gerth, 1990) Expansion of the goethite unit-cell along the b-direction indicates a distortion of Ni-O-OH octahedra along the b-axis (i e a lengthening of apical Ni-O bond distances relative to equatorial Ni-O/OH bond lengths) This is similar to the effect arising from incorporation of Mn^{3+} where differential lengthening of apical Mn-O bonds occurs as a consequence of the Jahn-Teller effect (Cornell and Giovanoli, 1987) The increase in the b-dimension of S1- and S2-goethites generally accounts for the increase in unit-cell volume as Ni substitution increases (Figure 2) consistent with incorporation of the larger Ni^{2+} ion (radius 0 69Å) relative to Fe^{3+} (0 65Å) (Table 2)

Table 1: *Unit-cell a- and c-dimensions for S1 and S2, pure and Ni-substituted goethites*

	S1-Goethites			S2-Goethites			
	a (Å)*	c (Å)*		a (Å)*	c (Å)*	a (Å)#	c (Å)#
Control C1	4.630 (0)	3.030 (0)	Control C1	4.637 (2)	3.021 (1)	4.623 (3)	3.022 (2)
Control C2	4.630 (2)	3.031 (0)	Control C2	4.643 (2)	3.016 (1)	4.629 (4)	3.022 (2)
Control C3	4.623 (0)	3.031 (0)	Control C3	4.623 (1)	3.025 (0)	4.630 (4)	3.021 (2)
3.0% Ni	4.628 (1)	3.030 (1)	2.7% Ni	4.641 (1)	3.018 (0)	4.621 (3)	3.021 (2)
5.0% Ni	4.645 (2)	3.024 (1)	3.9% Ni	4.624 (3)	3.023 (1)	4.623 (4)	3.021 (2)
6.6% Ni	4.631 (4)	3.030 (2)	4.5% Ni	4.631 (3)	3.022 (1)	4.623 (3)	3.021 (2)
10.0% Ni	4.625 (3)	3.028 (1)	5.0% Ni	4.632 (1)	3.023 (0)	4.619 (2)	3.024 (1)

Numbers in parentheses are the standard deviation of the last digit for unit-cell determinations.
* Unit-cell edge lengths were calculated from corrected positions of the 110, 130, 111 and 140 reflections.
\# Unit-cell edge lengths were calculated from corrected positions of the 020, 110, 120, 130, 021, 111, 121, 140, 160 and 250 reflections.

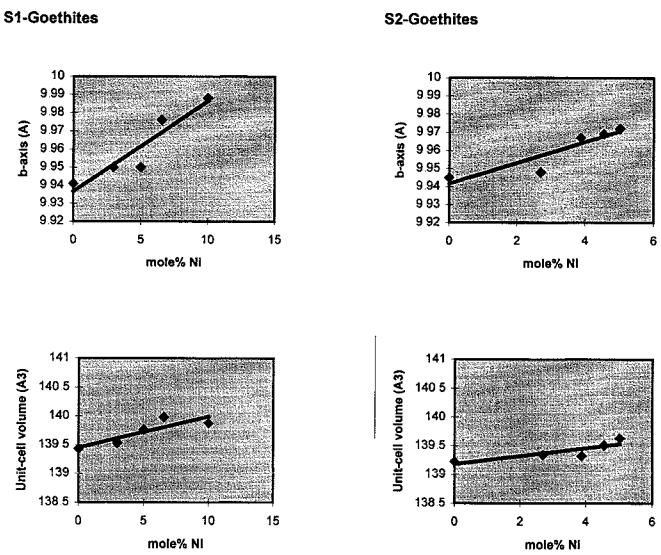

Figure 2: *Unit-cell b-dimension and unit-cell volume for S1- and S2-goethites, calculated from corrected positions of the 110, 130, 111 and 140 lines, versus mole% Ni substitution. Regression analysis: S1-goethites, (b_O), y = 9.937 + 4.94x10^{-3} % Ni (r^2 = 0.87**), (V_O), y = 139.45 + 0.055% Ni (r^2 = 0.77*); S2-goethites, (b_O), y = 9.942 + 5.77 x 10^{-3}% Ni (r^2 = 0.83**), (V_O), y = 139.18 + 0.069% Ni (r_2 = 0.72*).*

Golightly (1981) and Schellmann (1983) have suggested that Ni^{2+} incorporation in natural goethites may be coupled with Si^{4+}, for two Fe^{3+} ions within goethite, to compensate for the charge deficiency of Ni^{2+}. However, Si is only appreciably soluble at pH >9 and the coupled substitution of Ni^{2+} and Si^{4+} is not a suitable explanation for goethites prepared in the present study. Charge balance may be accounted for by the coupled substitution of Ni^{2+} and H^+ for Fe^{3+} within goethite. Schulze (1982) has proposed a defect goethite structure where Fe^{3+} ions are replaced by H^+ ions. This increases the protonation of hexagonally close-packed O atoms and is thought to account for the additional non-stoichiometric water that is commonly reported for natural and synthetic goethites (Kühnel *et al*, 1975; Schulze and Schwertmann, 1984).

Unit-cell parameters (i.e. a_O, c_O V_O) for Ni-hematites were linearly and positively related to increasing amounts of Ni substitution (Figure 3). This is consistent with the smaller Fe^{3+} ion being replaced by the larger Ni^{2+} ion (Table 2). Incorporation of Ni^{2+} within hematite may involve a mechanism similar to that described for Ni substituted goethites.

Unit-cell dimensions for Ni-hematites obtained by the calcination of precursive Ni-goethites at 300 and 800°C (Lim-Nunez, 1985) did not show a systematic trend with Ni-substitution and were generally less than dimensions of hematites observed in the present study (Figure 3). This may be a consequence of the increased crystallinity (i.e. structural ordering) and smaller excess water and OH content of Ni-hematites obtained by calcining precursive Ni-goethites as compared to hematite synthesized from ferrihydrites in this work.

MORPHOLOGY

Control S1 goethites, formed by the oxidative hydrolysis of Fe^{2+}, consisted of aggregated, 'cigar-shaped' or 'spindle-like' crystals with single and star-shaped twin forms approximately 300 x 1100 nm (n = 13) in size (Figure 4). Low Ni-goethites show a lath-like morphology (36 x 230 nm, n = 40) with stepped or serrated crystal terminations which suggests a multidomainic substructure, and reduced crystal growth along the b- and c-directions (i.e. width and length, respectively) relative to control goethites. Goethites with high Ni contents consisted of aggregated, sub-rounded to rounded particles about 40-60 nm (n = 4) in size.

The morphology of high-Ni S1-goethites is similar to the morphology reported for synthetic Al-goethites prepared from green-rusts (Weed *et al*, 1976; Mann *et al*, 1985). In the case of Al-substituted goethites, crystallization is thought to be inhibited by the presence of CO_3^{2-} similar to that occurring in Al-hydroxyl systems (Serna et al., 1977). A similar mechanism may occur for S1 Ni-goethites of the present study.

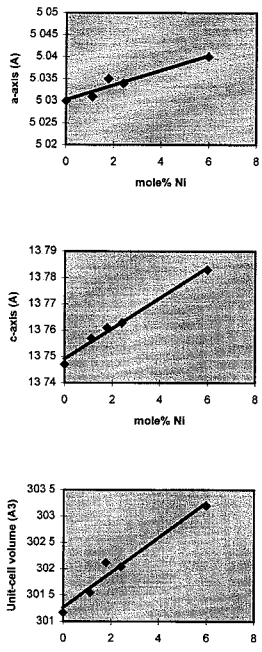

Figure 3: *Unit-cell parameters of Ni-hematites versus mole% Ni substitution Regression analysis (ao), y = 5 030 + 1.71x10^{-3}% Ni (r^2 = 0 93***), (c_O), y = 13 749 - 5 77x10^{-3}% Ni (r^2 = 0 986***), (V_O), y = 301 29 + 0 330% Ni (r^2 = 0 94***)*

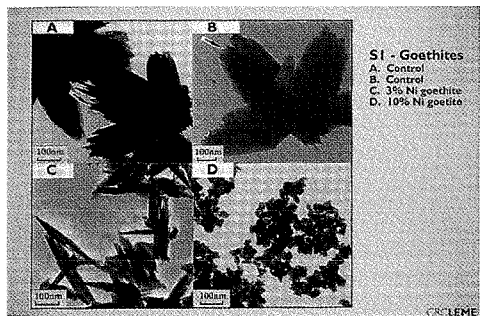

Figure 4: *Transmission electron micrographs of S1-goethites (A) Control, C1, (B) Control, C3 (C) 3.0 mole% Ni-substituted goethite and (D) 10 0 mole% Ni-substituted goethite Control goethites show stepped or serrated crystal terminations (A and B, arrowed)*

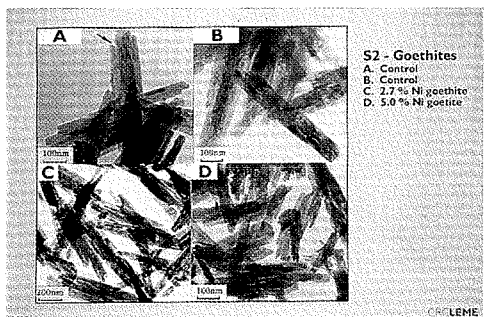

Figure 5: *Transmission electron micrographs of S2-goethites (A) Control, C1, (B) Control, C3, (C) 2 7 mole% Ni-substituted goethite and (D) 5.0 mole% Ni-substituted goethite Crystals show serrated or stepped terminations (A, arrowed)*

Control S2-goethites, formed by the alkaline hydrolysis of Fe^{3+}, show crystals with a raft or lath morphology, 130 x 610 nm (n = 26) in size, with stepped or serrated terminations (Figure 5) This is characteristic of synthetic goethite produced at high pH (Cornell *et al*, 1983; Schulze and Schwertmann, 1984) with crystals consisting of bundles of acicular, sub-units parallel to the c-direction (i e crystal length) and where unequal growth of these sub-units produce the stepped crystal terminations (Schulze and Schwertmann, 1984)

S2 goethites containing Ni retained the lath morphology (110 x 550 nm, n = 3) of the control goethites showing stepped or serrated terminations (Figure 5)

The well developed lath-like morphology of S2-goethites is not common for natural goethites but has been reported in the literature (Schwertmann and Latham, 1986; Amouric *et al*, 1986; Torrent *et al*, 1992) Goethite concentrated from soils and sediments typically consists of sub-rounded, plate-like crystals approximately 20 nm in size with no discernible, euhedral crystal morphology (Davey *et al*, 1975; Schwertmann and Latham, 1986; Anand and Gilkes, 1987; Torrent *et al*, 1992) The morphology of high-Ni S1-goethites (Figure 4D) is more typical of that reported for natural goethites

Low level Ni-substituted hematites consisted of pseudohexagonal, and predominantly subhedral particles, 135-160 nm (n = 20) in size, with stepped or lobed edges (Figure 6) Increasing Ni substitution produced more equant crystals about 120-140 nm (n = 20) in size Hematites produced in the present study are similar to rhombohedral hematites approximately 120-300 nm in size that were produced from ferrihydrite at pH 8-9 (Cornell and Giovanoli, 1989, 1993) This morphology is unlike that typically reported for natural hematites in soils where crystals are commonly reported to show a sub-rounded, plate-like habit (Davey et al, 1975; Anand and Gilkes, 1987), resembling natural goethites

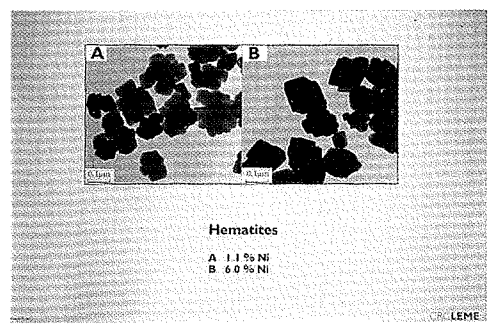

Figure 6: *Transmission electron micrographs of (A) low, and (B) high Ni-substituted hematites*

METAL DISTRIBUTION IN GOETHITE AND HEMATITE

Acid dissolution studies of natural and synthetic, metal-substituted Fe-oxides have been used as an indirect means of establishing cation substitution within goethite and hematite (Sidhu et al. 1980, 1981; Lim-Nunez and Gilkes, 1987). The technique is based on the assumption that dissolution of crystal faces is uniform in three dimensions and that crystals are of the same size and shape (Lim-Nunez and Gilkes, 1987). However, acid dissolution analysis should still reveal any major differences in the distribution of Ni within goethite and hematite.

Homogeneous incorporation of Ni requires that plots of % of total Ni dissolved versus % of total Fe dissolved give a straight line of unit slope intersecting the origin. Homogeneous cation (e.g. Ni) distribution within goethite and hematite is dependent on the constant relative adsorption of the metal and Fe^{3+} onto nucleation sites during crystallization. This condition is influenced, *inter alia*, by the various ionic properties of Ni including size, electronegativity and crystal field stabilization energy (CFSE) (Table 2). Upwardly convex or downwardly concave curves indicate inhomogeneous distribution towards the surface or centre of crystals, respectively.

Nickel within S1 goethites was more uniformly distributed than for S2 goethites, which showed accumulation of Ni towards the surface of crystals (Figure 7). Ionic size, electronegativity and ionic charge considerations appear to have outweighed the preference of Ni^{2+} over Fe^{3+} for octahedral positions (Table 2) resulting in surface accumulation of Ni within S2 goethites. S1 goethites, prepared from green-rust precursors, appear more able to accommodate Ni^{2+} than S2 goethites prepared from ferrihydrite. The near uniform distribution of Ni within S1 goethites may also be related to the simple Ni^{2+} (*aq*) species that exists under such conditions being more easily incorporated within goethite as compared to the high pH, $Ni_4(OH)_4^{4+}$ species which may have limited the extent of Ni-adsorption at the surface of goethite crystals.

Table 2: *Ionic sterochemistry of elements in octahedral coordination in oxides*

Ion	Electron Configuration	Effective ionic radius (Å)#	Electro-Negativity*	M-O bond Energy^ KJ/mol	Octahedral CFSE@ KJ/mol	Site Preference energy@ KJ/mol
Fe2+	3d6	0.61 (LS)[1] 0.78 (HS)[2]	1.5	-	-	-
Fe3+	3d5	0.55 (LS)[1] 0.645 (HS)[2]	1.8	390.4	0	0
Ni2+	3d8	0.69	1.8	382.0	123.8	95.4

\# Shannon (1976); * Stark and Wallace (1980)
^ CRC (1988). Bond energies are given relative to a standard temperature of 298K.
@ CFSE - crystal field stabilization energy (Burns, 1970).
1 LS = low spin.
2 HS = high spin.

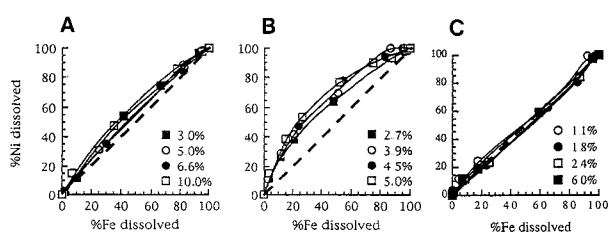

Figure 7: *Plots of % of total Ni dissolved versus % of total Fe dissolved for: (A) S1-goethites, (B) S2-goethites, and (C) hematites. Lines of unit-slope (- - - - -) indicate a uniform distribution of Ni within crystals of goethite and hematite.*

Nickel was uniformly distributed within hematite (Figure 7) and appeared to be more accommodating of Ni than goethite for similar levels of substitution. In marked contrast to this result, Sidhu *et al* (1980) reported that Ni was heterogeneously distributed within hematite occurring mostly at the surface of crystals. This difference in uniformity of substitution between the studies may be related to the calcination at 650°C of Ni-hematites by Sidhu *et al* (1980). Nickel substituted magnetites were converted to Ni-hematites via an intermediate Ni-maghemite phase. Surface concentration of Ni may be a consequence of the greater crystallinity of heat treated hematite so that the structure is less accommodating of Ni than is Ni-hematite derived from ferrihydrite. In addition, the spinel structure of magnetite and maghemite can accommodate much Ni^{2+}, which is not readily accommodated by hematite so that Ni^{2+} will have diffused to the surface of crystals during the high temperature transformation magnetite → maghemite → hematite.

Investigations of the dehydroxylation of synthetic Al-substituted goethites have shown that depending on the initial amount of Al in the parent goethite and temperature, Al can be retained in the transformed hematite (DeGrave *et al* 1988; Wells *et al* 1989). It would be expected in weathering profiles that during the dehydration of Ni-substituted goethite to hematite Ni would be retained in the structure of hematite. This aspect however, was not investigated in the present study and is worthy of further research.

SUMMARY AND CONCLUSIONS

Acid dissolution studies provided indirect evidence for the incorporation of Ni within goethite and hematite which was confirmed directly by x-ray diffraction (XRD). The unit-cell b-dimension and volume of S1- and S2-goethites, and the a- and c-dimensions of hematite increased as the level of Ni substitution increased. This was due to the replacement of Fe^{3+} by the larger Ni^{2+} ion. The mechanism of Fe^{3+} replacement may involve the paired substitution of Ni^{2+} and H^+ which is consistent with an increase in H_2O content for goethite (Kühnel *et al* 1975; Schulze and Schwertmann, 1984), although this was not confirmed in the present study.

The extent and homogeneity of Ni substitution within goethite is strongly influenced by the conditions of synthesis. At high pH some surface concentration of Ni occurred within goethite containing up to 6 mole%. Goethite synthesized at near neutral pH uniformly incorporated up to 10 mole% Ni. The size and shape of goethite crystals produced by the oxidation of mixed Fe^{2+}-Ni^{2+}-complexes closely resembled the morphology reported for natural goethites and the conditions of synthesis used are similar to those likely to occur in weathered profiles including Ni-laterite deposits. Nickel was uniformly incorporated to about 6 mole% within hematite.

Goethite and hematite can, therefore, be significant hosts of Ni mineralization in lateritic nickel deposits. Other iron-oxides occurring in Ni-laterites, such as maghemite which have been overlooked as a Ni source, may also contain significant amounts of Ni. Future research of the genesis of Ni-laterite deposits may also consider the goethite:hematite ratio and Al-substitution which, in a pedological context, has been used as an indicator of the conditions of soil formation (Fitzpatrick and Schwertmann, 1982; Fitzpatrick, 1988). In this case, relative amounts of goethite and hematite, and levels of Ni-substitution may provide information on the conditions of formation of Ni-laterites.

REFERENCES

Amouric, M., Baronet, A., Nahon, D. and Didier, P. (1986). Electron microscopic investigations of iron oxyhydroxides and accompanying phases in lateritic iron-crust pisolites. Clays and Clay Minerals 34, 45-52.

Anand, R. R. and Gilkes, R. J. (1987). Iron oxides in lateritic soils from Western Australian. Journal of Soil Science 38, 607-622.

Baes, Jr., C. F. and Mesmer, R. E. (1976). The hydrolysis of cations. John Wiley and Sons, pp489.

Bernal, J. D., Dasgupta, D. R. and Mackay, A. L. (1959). The oxides and hydroxides of iron and their structural inter-relationships. Clay Minerals Bulletin 4, 15-30.

Bernstein, L. and Waychunas, G. A. (1987). Germanium crystal chemistry in hematite and goethite from the Apex mine, Utah, and some data on germanium in aqueous solution and in stottite. Geochimica et Cosmochimica Acta 51, 623-630.

Burger, P. A. (1996). Origins and characteristics of lateritic deposits. In: Proceedings Nickel '96, pp 179-183. The Australasian Institute of Mining and Metallurgy, Melbourne.

Burns, R G (1970) Mineralogical applications of crystal field theory Cambridge Press, pp224

Cornell, R M and Giovanoli, R (1987) Effect of manganese on the transformation of ferrihydrite into goethite and jacobsite in alkaline media Clays and Clay Minerals 35, 11-20

Cornell, R M and Giovanoli, R (1989) The effect of cobalt on the formation of crystalline iron oxides from ferrihydrite into goethite and hematite in alkaline media Clays and Clay Minerals 37, 65-70

Cornell, R M and Giovanoli, R (1993) Acid dissolution of hematites of different morphologies Clay Minerals 28, 223-232

Cornell, R M , Posner, A M and Quirk, J P (1974) Crystal morphology and the dissolution of goethite Journal of Inorganic and Nuclear Chemistry 36, 1937-1946

Cornell, R M , Mann, S and Skarnulis, A J (1983) A high resolution electron microscopy examination of domain boundaries in crystals of synthetic goethite Journal Chemical Society Faraday Transactions 1, 2679-2684

Cotton, F A and Wilkinson, G (1980) Advanced inorganic chemistry: A comprehensive text 4th ed , Wiley, New York, pp 1396

CRC (1988) Handbook of Chemistry of Physics, 1st Student Edition, Robert Weast (ed), CRC Press Inc , Florida

Davey, B G , Russell, I D and Wilson, M J (1975) Iron oxides and clay minerals and their relationship to colours of red and yellow podzolic soils near Sydney, Australia Geoderma 14, 125-138

DeGrave, E , Bowen, L H , Amarasiriwarden, D D and Vandenberghe, R E (1988) 57Fe Mössbauer effect study on highly substituted aluminium hematites: Determination of the magnetic hyperfine field distributions Journal of Magnetism and Magnetic Materials 72, 129-140

Elias, M , Donaldson, M J and Giorgetta, N (1981) Geology, mineralogy and chemistry of lateritic nickel-cobalt deposits near Kalgoorlie, Western Australia Economic Geology 76, 1775-1783

Fischer, W R and Schwertmann, U (1975) The formation of hematite from amorphous iron (III) hydroxide Clays and Clay Minerals 23, 33-37

Fitzpatrick, R W (1988) Iron compounds as indicators of pedogenic processes: Examples from the southern hemisphere In: Iron in Soils and Clay Minerals, J W Stucki et al (eds), Reidel Publishing Co pp 351-396

Fitzpatrick, R W and Schwertmann, U (1982) Al-substituted goethite, an indicator of pedogenic and other weathering environments in South Africa Geoderma 27, 335-347

Fitzpatrick, R W , le Roux, J and Schwertmann, U (1978) Amorphous and crystalline titanium and iron-titanium oxides in synthetic preparations, at near ambient conditions, and in soil clays Clays and Clay Minerals 26, 189-201

Gasser, U G , Jeanray, E , Mustin, C , Barres, O , Nüesch, R , Berthelin, J and Herbillon, A J (1996) Properties of synthetic goethite with Co for Fe substitution Clay Minerals 31, 465-476

Gerth, J (1990) Unit-cell dimensions of pure and trace metal-associated goethites Geochimica et Cosmochimica Acta 54, 363-371

Giovanoli, R and Cornell, R M (1992) Crystallization of metal-substituted ferrihydrites Zeitschrift fuer Pflanzenernaehrung und Bodenkunde 129, 63-77

Golightly, J P (1979) Nickeliferous laterites: A general description In: Evans, D J I , Shoemaker, R S and Veltman, H (eds), International Laterite Symposium, AIME New York, 3-23

Golightly, J P (1981) Nickeliferous laterite deposits Economic Geology, 75th Anniversary Volume, 710-735

Kühnel R A (1975) The role of cationic and anionic scavengers in laterite Chemical Geology 60, 31-40

Kühnel, R A , Roorda, H J and Steensma, J J (1975) The crystallinity of minerals - A new variable in pedogenic processes: A study of goethite and associated silicates in laterites Clays and Clay Minerals 23, 349-354

Lim-Nunez, R (1985) Synthesis and acid dissolution of metal-substituted goethites and hematites MSc Thesis, University of Western Australia, pp 223

Lim-Nunez, R. and Gilkes, R. J. (1987) Acid dissolution of synthetic metal-containing goethites and hematites. In: Proceedings of the International Clay Conference, Denver, 1985. Schulzt, L. G., van Olphen, H. and Mumpton, F. A., eds. The Clay Minerals Society, Bloomington, Indiana, pp. 197-204.

McKeague, J. A. and Day, J. H. (1966). Dithionite- and oxalate-extractable Fe and Al as aids in differentiating various classes of soils. Canadian Journal of Soil Science 46, 13-22.

Mann, S., Cornell, R. M. and Schwertmann, U. (1985) The influence of aluminium on iron oxides: XII. High resolution transmission electron microscopic (HRTEM) study of aluminous goethites. Clay Minerals 20, 255-262.

Nahon, D., Paquet, H. and Delvigne, J. (1982). Lateritic weathering of ultramafic rocks and the concentration of nickel in the western Ivory Coast. Economic Geology 77, 1159-1175.

Norrish, K. (1975) Geochemistry and mineralogy of trace elements. In: Trace elements in the soil-plant-animal system. Nicholas, A. R. and Egan, D. J. (eds.), Academic Press.

Novak, G. A. and Colville, A. A. (1989) A practical interactive least-squares cell-parameter program using an electronic spreadsheet and a personal computer. American Mineralogist 74, 488-490.

Parfitt, R. L. (1989) Optimum conditions for extraction of Al, Fe and Si from soils with acid oxalate. Communications in Soil Science and Plant Analysis 20, 801-816.

Peña, F. and Torrent, J. (1984) Relationships between phosphate sorption and iron oxides in Alfisols from a river sequence of Mediterranean Spain. Geoderma 33, 283-296.

Schellmann, W. (1983) Geochemical principles of lateritic nickel ore formation. In: Melfi, A. J. and Carvalho, A. (eds.), II International Seminar on Lateritisation Processes. University of Sao Paulo Press, San Paulo, pp. 119-135.

Schulze, D. G. (1982). The x-ray identification of iron oxides by differential x-ray diffraction and the influence of aluminium substitution on the structure of goethite. PhD. Thesis, Technishe Universitat, Munchen. Fed. R. Germany.

Schulze, D. G. (1984) The influence of Al on iron oxides. VIII. Unit-cell dimensions of Al-substituted goethites and estimation of Al from them. Clays and Clay Minerals 32, 36-44.

Schulze, D. G. and Schwertmann, U. (1984) The influence of aluminium on iron oxides. XIII. Properties of goethite synthesized in 0.3M KOH at 25°C. Clay Minerals. 22, 83-92.

Schwertmann, U. (1964) The differentiation of iron oxides in soils by a photochemical extraction with acid ammonium oxalate. Zeitschrift fuer Pflanzenernaehrung und Bodenkunde 105, 194-202.

Schwertmann, U. and Latham, M. (1986). Properties of iron oxides in some New Caledonian oxisols. Geoderma 39, 105-123.

Schwertmann, U. and Fischer, W. R. (1966) Zur Bilding von a-FeO.OH und α-Fe_2O_3 aus amorphen Eisen-(III) hydroxide. Zeitschrift fuer Anorganische und Allgemeine Chemie 346, 137-142.

Schwertmann, U. and Fischer, W. R. (1973) Natural amorphous ferric hydroxide. Geoderma 10, 237-247.

Schwertmann, U. and Pfab, G. (1994) Structural vanadium in synthetic goethite. Geochimica et Cosmochimica Acta 58, 4349-4352.

Schwertmann, U., Gasser, U. and Sticher, H. (1989) Chromium-for-iron substitution in synthetic goethites. Geochimica et Cosmochimica Acta 53, 1293-1297.

Serna, C. J., White, J. L. and Hem, S. L. (1977). Anion-aluminium hydroxide gel interactions. Soil Science Society of America Journal 41, 1009-1013. Sidhu, P. S., Gilkes, R. J. and Posner, A. M. (1980) The behaviour of Co, Ni, Zn, Cu, Mn and Cr in magnetite during alteration to maghemite and hematite. Soil Science Society of America Journal 44, 135-138.

Sidhu, P. S., Gilkes, R. J., Cornell, R. M., Posner, A. M. and Quirk, J. P. (1981) Dissolution of iron oxides and oxyhydroxides in hydrochloric and perchloric acids. Clays and Clay Minerals 29, 269-276.

Shannon, R. D. (1976). Revised effective ionic radii and systematic studies of inter-atomic distances in halides and chalcogenides. Acta Crystallographica A32, 751-767.

Stark, J. G. and Wallace, H. G. (1980). Chemistry data book, SI edition. Fakenham Press Ltd., Fakenham, Norfolk, pp. 112.

Stiers, W and Schwertmann, U (1985). Evidence for manganese substitution in synthetic goethite. Geochimica et Cosmochimica Acta 49, 1909-1911.

Taylor, R M and McKenzie, R M (1980) The influence of aluminium on iron oxides VI. The formation of Fe(II)-Al(III) hydroxy-chlorides, -sulphates and -carbonates as new members of the pyroaurite group and their significance in soils. Clays and Clay Minerals 28, 179-187

Torrent, J , Schwertmann, U and Barron, V (1992) Fast and slow phosphate sorption by goethite-rich natural materials Clays and Clay Minerals 40, 14-21

Weed, S B , Golden, D C and Bigham, J M (1976) Properties of aluminium substituted goethite Agronomy Abstracts 1976, pp133

Wells, M A , Gilkes, R J and Anand, R R (1989). The formation of corundum and aluminous hematite by the thermal dehydroxylation of aluminous goethite Clay Minerals 24, 513-530